Available online at www.sciencedirect.com
ScienceDirect
Polyhedron 26 (2007) 3783–3792
POLYHEDRON
www.elsevier.com/locate/poly

Transition metal complexes with thiosemicarbazide-based ligands. Part LVI: Nickel(II) complex with 1,3-diphenylpyrazole-4-carboxaldehyde thiosemicarbazone and unusually deformed coordination geometry

Vukadin M. Leovac [a], Slađana B. Novaković [b], Goran A. Bogdanović [b], Milan D. Joksović [c,*], Katalin Mészáros Szécsényi [a], Valerija I. Češljević [a]

[a] *Faculty of Sciences, University of Novi Sad, Trg D.Obradovića 3, 21000 Novi Sad, Serbia*
[b] *VINČA Institute of Nuclear Sciences, P.O. Box 522, Belgrade 11001, Serbia*
[c] *Faculty of Sciences, University of Kragujevac, R. Domanovica 12, 34000 Kragujevac, Serbia*

Received 6 February 2007; accepted 6 April 2007
Available online 27 April 2007

Abstract

Synthesis of a new nickel(II) complex, $[Ni(Ph_2PzTSC\text{-}H)_2]$ with 1,3-diphenylpyrazole-4-carboxaldehyde thiosemicarbazone (Ph_2PzTSC), is described. The compounds have been characterized by elemental and thermal analysis, molar conductivity and spectral (UV–Vis, IR, ^1H NMR, and ^{13}C NMR) measurements. In the case of complex the magnetic measurement has been also performed. Crystal and molecular structures of both the free ligand and the complex have been determined by single crystal X-ray analysis. It was found that the ligand coordinates in a bidentate NS fashion, in its deprotonated thioenolato form. The *cis*-square-planar geometry of the complex is significantly distorted tetrahedrally. The Cambridge Structural Database (CSD) study has been performed to obtain geometrical and structural informations on similar nickel(II) complexes in order to compare structural data.

Keywords: Nickel(II) complex; Thiosemicarbazone; Spectroscopic and TA studies; Crystal structure; CSD study

1. Introduction

A number of *N*-heterocyclic thiosemicarbazones and their metal ion complexes have attracted considerable interest in chemistry and biology, owing to their potentially beneficial biological activities (antibacterial, antimalarial, antiviral, etc.), which have often been related to a chelation phenomenon with trace of metal ions [1–5]. Heterocyclic thiosemicarbazones are believed to exercise their beneficial therapeutic properties in mammalian cells by inhibiting ribonucleotide reductase in the synthesis of DNA precursors [4].

On the other side, many pyrazole derivatives are known to exhibit also a wide range of biological properties. Particularly, arylpyrazoles are important in medicinal and pesticidal chemistry [6]. Recently, some arylpyrazoles were reported to have non-nucleoside HIV-1 reverse transcriptase inhibitory activity [7]. Extensive studies have been devoted to arylpyrazole derivatives such as Celecoxib, a well-known cyclooxygenase-2 inhibitor [8–11]. More recently, pyrazole derivatives as high affinity and selective A2B adenosine receptor antagonists have been reported [12].

The well-documented biological activities of *N*-heterocyclic thiosemicarbazones have prompted further investigation on the coordination chemistry of such ligands during the last period [5,13] with the recommendation that

* Corresponding author. Tel.: +381 34336223; fax: +381 34335040.
E-mail address: mjoksovic@kg.ac.yu (M.D. Joksović).

0277-5387/$ - see front matter © 2007 Elsevier Ltd. All rights reserved.
doi:10.1016/j.poly.2007.04.012

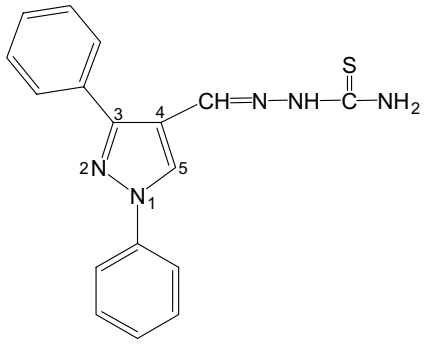

Fig. 1. Chemical structure of Ph_2PzTSC.

structural variation on the heterocyclic ring might bring out significant enhancement in their biological effects, especially in corresponding metal complexes, often with novel structural information. Synthesis and spectroscopic characterization of nickel(II) complexes with some pyrazolyl thiosemicarbazones, such as 5-methyl-3-formylpyrazole-3-substituted thiosemicarbazones have been reported by other authors [14–16]. As a part of our investigation toward synthesis and structural characterization of new compounds containing biorelevant pyrazolyl thiosemicarbazones, the present paper reports the synthesis, spectroscopic, and structural properties of 1,3-diphenylpyrazole-4-carboxaldehyde thiosemicarbazone ligand (Ph_2PzTSC, Fig. 1) and its nickel(II) complex.

2. Experimental

2.1. Reagents and starting materials

Solvents and reagents were obtained from commercial sources. The solvents were purified using the established method [17]. Thiosemicarbazide and nickel(II) acetate tetrahydrate were purchased from Aldrich Chemicals, USA. 1,3-Diphenylpyrazole-4-carboxaldehyde was synthesized according to Rathelot et al. procedure [18].

2.2. Preparation of Ph_2PzTSC

The Ph_2PzTSC ligand was prepared by refluxing the mixture of the 1,3-diphenylpyrazole-4-carboxaldehyde (1.24 g, 5 mmol) and thiosemicarbazide (0.45 g, 5 mmol) in ethanol (20 cm^3) for 4 h. One drop of glacial acetic acid was previously added into the mixture. After cooling, the white precipitate was filtered, washed with cold chloroform in order to remove the traces of unchanged aldehyde, and dried over anhydrous calcium chloride. Yield: 1.25 g, 78%. The suitable crystals for X-ray analysis were obtained by recrystallization of the ligand from the mixture of acetone and methanol (1:1 v/v).

Anal. Calc. for $C_{17}H_{15}N_5S$: C, 63.53; H, 4.70; N, 21.79. Found: C, 63.75; H, 4.62; N, 21.55%. UV–Vis spectra (cm^{-1}/log ε): 31950 (4.0); ~30 000 (4.0).

^1H NMR (200 MHz, DMSO-d_6): 7.38–7.70, m (8H, Ar); 7.80, br s (1H, NH_2); 7.90, d (2H, Ar, $J = 7.86$ Hz, *ortho*-H, N-substituted phenyl); 8.22, s (1H, Pz); 8.27, br s (1H, NH_2); 9.19, s (1H, CH=N); 11.34, br s (1H, NH).

^{13}C NMR (200 MHz, DMSO-d_6): 117.43; 118.66; 127.15; 127.85; 128.30; 128.75; 128.91; 129.85; 132.28; 135.10; 139.20; 151.52; 177.72.

IR (KBr pellets): 3326, 3257, 3140, 1618, 1598, 1543, 1500, 1221, 1098, 1064, 831, 807, 755, 704, 687 cm^{-1}.

2.3. Preparation of $[Ni(Ph_2PzTSC\text{-}H)_2]$

$Ni(CH_3COO)_2 \cdot 4H_2O$ (0.25 g, 1 mmol) was dissolved in methanol (10 cm^3) under heating and the solution was mixed with a warm solution of Ph_2PzTSC (0.32 g, 1 mmol) in acetone (20 cm^3). The heating was continuated for several minutes. After 10 h of standing, the brown crystals were filtered and washed with acetone and dried over anhydrous calcium chloride Yield: 0.16 g, 46%.

Anal. Calc. for $C_{34}H_{28}N_{10}NiS_2$: C, 58.38; H, 4.03; N, 20.02; Ni, 8.39. Found: C, 58.42; H, 3.98; N, 20.12; Ni, 8.42%. $\lambda_M(DMF) = 3.3$ S cm^2 mol^{-1}. UV–Vis: (cm^{-1}/log ε): ~33 300 (4.0); 30 210 (4.3); 25 500 sh (3.7); 19 300 sh (2.1). sh (shoulder).

^1H NMR (200 MHz, DMSO-d_6): 6.97–7.19, m (7H; 5H, phenyl and 2H, NH_2); 7.49, s (1H, Pz); 7.50, d (1H, Ar, $J = 7.36$Hz, *para*-H, N-substituted phenyl); 7.65, t, (2H, Ar, $J = 7.66$Hz, *meta*-H, N-substituted phenyl); 8.03, d, (2H, $J = 7.77$Hz, *ortho*-H, N-substituted phenyl); 9.84, s (1H, CH=N, azomethine).

^{13}C NMR (200 MHz, DMSO-d_6): 114.29; 119.89; 127.62; 127.86; 128.44; 128.83; 129.88; 130.10; 130.89; 139.23; 150.17; 152.68; 173.46.

IR (KBr pellets): 3466, 3284, 3067, 1626, 1596, 1526, 1513, 1504, 1219, 956, 705, 672 cm^{-1}.

2.4. Physical measurements

Elemental (C, H, N) analysis of the samples was carried out by standard micromethods in the Center for Instrumental Analysis, Faculty of Chemistry, Belgrade. Nickel content was determined by the complexometric titration with EDTA method, upon the destruction of complex with the mixture of concentrated H_2SO_4 and HNO_3. Molar conductivity of freshly prepared 1×10^{-3} mol dm^{-3} solution was measured on a Jenway 4010 conductivity meter. IR spectra were recorded on a Perkin Elmer Spectrum One FT-IR spectrometer with a KBr disc. ^1H and ^{13}C NMR spectra were obtained using a Varian Gemini 200 spectrometer. Electronic spectra were recorded on a Secomam (Anthelie 2, Advanced, for the range 270–900 nm) and on a Thermo Nicolet instrument (NEXUS 670 FT-IR, for the range 900–1400 nm) in $(1–2) \times 10^{-3}$ mol dm^{-3} DMF solutions of the ligand and complex. Thermal analysis in argon and air gas carriers with a 15 dm^3/min flowing rate and a heating rate of 10 K/min were carried out using a DuPont 1090 TA system. For thermogravimetric

measurements platinum crucible was employed. DSC curves were recorded in open aluminum sample pans. As a reference an empty pan was used. The sample masses were about 5 mg.

2.5. X-ray data collection and structure refinement

The diffraction data for both compounds were collected on an Enraf-Nonius CAD4 diffractometer [19] by using graphite-monochromated Mo Kα (0.71073 Å) radiation at 293(2) K. The data were corrected for Lorentz and polarization effects [20]. Cell constants and the orientation matrix for data collection, obtained from 25 centered reflections in the θ range of 13.17–15.81° for the ligand, corresponded to an orthorhombic cell. In the case off the complex, the 25 centered reflections in the θ range 13.97–17.25° led to a triclinic cell. Both structures were solved by direct methods and difference Fourier methods and refined on the F^2 by full-matrix least-square method [21]. In both cases the all H atoms were determined from ΔF maps but at the final stage of the refinement they were placed at geometrically calculated positions (in purpose to decrease the number of refined parameters). The calculated C–H and N–H distances were 0.93 and of 0.86 Å respectively, and the isotropic displacement parameters are equal to 1.5 and 1.2 times of the equivalent isotropic displacement parameters of the C and N atoms. The software used for the publication are: PLATON [22], WinGX [23], PARST [24] and ORTEPIII [25]. Crystal and structure refinement data for Ph_2PzTSC and $[Ni(Ph_2PzTSC\text{-}H)_2]$ are summarized in Table 1.

Table 1
Crystal and structure refinement data for Ph_2PzTSC and $[Ni(Ph_2PzTSC\text{-}H)_2]$

Empirical formula	$C_{17}H_{15}N_5S$	$C_{34}H_{28}N_{20}NiS_2$
Formula weight	321.40	699.49
Color	white	brown
Temperature (K)	293(2)	293(2)
Crystal size (mm)	$0.025 \times 0.014 \times 0.010$	$0.300 \times 0.026 \times 0.020$
Crystal system	orthorhombic	triclinic
Space group	*Pbca*	$P\bar{1}$
Unit cell		
a (Å)	8.458(4)	12.364(6)
b (Å)	17.476(6)	12.451(5)
c (Å)	21.986(5)	12.478(5)
α (°)	90	103.27(4)
β (°)	90	92.86(6)
γ (°)	90	115.59(3)
Volume (Å^3)	3249.8(14)	1661.7(12)
Z	8	2
Calculated density, ρ (g cm^{-3})	1.314	1.398
θ Range for data collection (°)	1.58–25.97	2.44–25.98
Absorption coefficient (mm^{-1})	0.206	0.751
$F(000)$	1344	724
Index ranges	$0 \leqslant h \leqslant 10$, $0 \leqslant k \leqslant 21$, $0 \leqslant l \leqslant 27$	$0 \leqslant h \leqslant 15$, $-15 \leqslant k \leqslant 14$, $-15 \leqslant l \leqslant 15$
Reflections collected	3617	6832
Independent reflections	3617	6511
Parameters	208	424
Goodness-of-fit	0.914	1.004
R_1 [$I > 2\sigma(I)$]	0.0636	0.0472
Largest difference in peak and hole	0.273 and −0.241	0.383 and −0.338

3. Results and discussion

3.1. Syntheses and general properties of ligand and complex

The title ligand, 1,3-diphenylpyrazole-4-carboxaldehyde thiosemicarbazone (Ph_2PzTSC) was synthesized in good yield (78%) by condensation from warm ethanolic solutions of the corresponding aldehyde and thiosemicarbazide in an 1:1 mole ratio, in the presence of a small quantity of the glacial acetic acid. The white crystals of the ligand are stable at room temperature. The ligand is very soluble in Me_2CO and DMF, soluble in MeOH, less soluble in aqueous EtOH, and practically insoluble in Et_2O and water.

The brown single crystals of the *cis*-square-planar $[Ni(Ph_2PzTSC\text{-}H)_2]$ complex were obtained by reaction of the warm methanolic solution of $Ni(CH_3COO)_2 \cdot 4H_2O$ with acetone solution of the ligand in mole ratio of 1:1. The complex is soluble in DMF, less soluble in Me_2CO, and insoluble in Et_2O, MeOH, EtOH, and water.

The ligand participates in coordination with nickel(II) ion in its monoanionic form after deprotonation of the hydrazine nitrogen, due to the presence of acetate ion as a Brönsted base, resulting in complex of non-electrolyte type. This is in the agreement with its low molar conductivity. The diamagnetism of the complex is in the accordance with its square-planar structure confirmed by X-ray analysis. The diamagnetic property of the complex is also retained in DMF solution.

3.2. IR spectral studies

A comparative study of the IR spectral data of the complex with that of the ligand gives valuable information regarding bonding sites of the ligand molecule.

The IR spectra of compounds with C=S group attached to a nitrogen show an absorption band due to ν(C=S) stretching in the region between 1020 and 1250 cm^{-1}. In principle, the ligand can exhibit thione/thiol tautomerism, since it contains a thioamide NH–C=S functional group [26]. The missing ν(S–H) band between 2600 and 2800 cm^{-1} indicates that the ligand remains in its thione form. The ligand exhibits a strong band at 1098 and a medium one at 1064 cm^{-1} due to ν(C=S) stretches [27]. Also, two bands at 831 and 807 cm^{-1} in the spectrum of the free ligand can be attributed to vibrations involving interaction between ν(C=S) stretching and ν(C–N) stretchings [28]. The appearance of these bands indicates the existence of ligand in its thione form in the solid state. The disappear-

ance of the ν(C=S) band in this region and the appearance of a medium intensity band at 672 cm^{-1} in the spectrum of the complex suggests the thioenolization of the C=S group and coordination of the thiolate sulfur to nickel [29].

In the spectrum of the ligand three bands appear in the frequency range 3000–4000 cm^{-1}. Two of them, at 3327 and 3257 cm^{-1}, belong to are due to asymmetrical and symmetrical $\nu(NH_2)$ stretching, respectively, and one to the hydrazine ν(NH) at 3159 cm^{-1} [30]. The spectral ν(N–H) band of thiosemicarbazone disappears in the complex indicating the deprotonation of the NH group and coordination via the thiolate sulfur. On the other hand, the bands in the region attributed to symmetrical and asymmetrical stretching modes $\nu(NH_2)$ in the spectrum of the ligand, undergo a change in the spectrum of the complex. This is explained by the coordination of sulfur from C=S(NH_2) group as reported earlier [31,32].

In the ligand spectrum, the strong band observed at 1618 cm^{-1} is assigned to ν(C=N) stretching vibrations [33]. This band shifts to higher wavenumbers at 1626 cm^{-1} in the spectrum of the complex, indicating the coordination of nitrogen of the azomethine group to the central metal ion [31,34].

According to the literature data [15,16], IR bands assigned to $\nu(C{=}N_{pz})$ (pyrazole ring) have been found to shift to the higher frequency region in the nickel complexes referring to the participation of the ring nitrogen atom as a potential bonding site. The negative shift of the very strong $\nu(C{=}N_{pz})$ frequencies from 1543 cm^{-1} in the spectrum of the free Ph_2PzTSC to 1526 cm^{-1} after complexation with nickel(II) ion does not indicate the involvement of pyrazole nitrogen in bonding. This band shifting to lower wavenumbers could be explained by resonance effects through the all conjugated system after the deprotonation and complexation with nickel(II) ion.

3.3. NMR spectral studies

The assignment of all reported signals (^{1}H and ^{13}C) was carried out by means of 1D and 2D homo- and heteronuclear correlated NMR spectroscopy.

3.3.1. ^{13}C NMR spectra

The carbon C=S signal appears at higher field in the spectrum of the complex compared to that in the ligand. This behavior suggests thione-to-thiol evolution in the ligand, an increase in the thiocarbonyl-deprotonated nitrogen bond order [35] and possible coordination of the nickel ion to the thiolic sulfur atom.

^{13}C NMR spectrum shows an unexpectedly low positive $\Delta\delta = \delta$(complex) − δ(free ligand) shift of only 2.0 ppm for the azomethine carbon. In the earlier reports, the complexation through azomethine nitrogen causes a great positive chemical shift of the azomethine carbon in the ^{13}C NMR spectra of complexes [35,36]. On the other side, the C-5 pyrazole carbon exhibits a great positive shift of 15.0 ppm, while the C-4 carbon is shifted to higher field for 3.1 ppm. This behavior of the C-5 pyrazole carbon is probably caused by the positive resonance effect of the phenyl-substituted pyrazole nitrogen, due to the delocalization of π-electrons through C-5, C-4, azomethine carbon, and thiosemicarbazone part of the molecule after the deprotonation of hydrazine nitrogen and complexation. Thus, the reduced electron density of the azomethine carbon after coordination is compensated by resonance effect which results in low difference in the chemical shift of the azomethine carbon in the spectrum of the free ligand compared to that in the complex. In this way the electron density of the azomethine nitrogen is significantly increased as well as its nucleophility facilitating its coordination to nickel(II). The practically same δ-value for C-3 pyrazole carbon (139.2 ppm) in the ^{13}C NMR spectrum of the free ligand compared to the corresponding shift in the complex confirms this hypothesis. The chemical shifts of the other carbon atoms undergo no significant changes upon complexation.

3.3.2. ^{1}H NMR spectra

The ^{1}H NMR spectrum of Ph_2PzTSC ligand show a broad singlet at 11.34 ppm relative to the NH next to C=S, while the signal of the azomethine proton appears at 9.19 ppm. The sharp singlet of the pyrazole proton appears at 8.22 ppm while the aromatic protons occur in 7.38–7.92 ppm range. It is interesting to notice the presence of two broad singlets for two NH_2 protons, at 8.27 and 7.80 ppm respectively. These two protons are different which means that the free rotation around C–N bond is hindered because of its partial double bond character [37].

The coordinating mode of the ligand was confirmed by comparing ^{1}H NMR spectral data of the ligand with the corresponding ones in the complex. The absence of the NH proton signal in the spectrum of the complex suggests the thioenolization and subsequently, the replacement of a proton by the metal ion. This replacement with nickel(II) induces the shift of NH_2 protons to lower δ-values in the spectrum of the complex (overlapped with the aromatic protons shifts in 6.97–7.19 ppm region).

A significant downfield shift of the azomethine proton signal in the complex ($\Delta\delta = 0.65$ ppm) with respect to the corresponding free ligand confirms the coordination of azomethine nitrogen [15,27].

It is interesting to emphasize that C-5 pyrazole proton shifts to lower δ-value from 8.22 ppm in the spectrum of the ligand to 7.49 ppm in the spectrum of the complex. On the other hand, the doublet assigned to *ortho*-N-substituted phenyl protons at 7.90 ppm (center of doublet) is shifted to lower field in the spectrum of the complex at 8.03 ppm, together with *meta* and *para* protons. These shifts are induced by positive resonance effect of phenyl-substituted pyrazole nitrogen and the participation of its electron pair in the delocalization of π-electrons after coordination, which is in the accordance with ^{13}C NMR spectral data for the free ligand and its nickel complex. The

other aromatic proton shifts of the ligand and those in the complex appear in the expected region.

3.4. Electronic spectra

Similarly to the ligand, the red-brownish DMF solution of the Ni(II) complex absorbs in the UV range in several unresolved bands belonging to intraligand transitions. A shoulder appearing at about 25 500 cm^{-1} is probably CT band.

The only one d–d band at about 19 000 cm^{-1} appearing as a shoulder of this CT band is consistent with the assumption of a preserved square-planar geometry in DMF solution. In the near IR region, under 10 000 cm^{-1} no bands were observed, as is usual in complexes with this geometry [38].

3.5. Crystal structures

3.5.1. Crystal structure of Ph_2PzTSC

Fig. 2. shows an ORTEP plot of Ph_2PzTSC ligand with the atomic numbering scheme. Relevant bond distances and angles are listed in Table 2. The thiosemicarbazone moiety of the ligand shows E configuration around the C2–N1 and C1–N2 bond as found in most of the thiosemicarbazones. As confirmed by the C=S bond distance of 1.692(5) Å, the ligand is present in its thione form. The partial double bond characters in formally single bonds of thiosemicarbazone moiety suggest the extensive electron delocalization. Consequently, this part of molecule exhibits considerable planarity. The moiety comprising C2, N1, N2, C1, S1, and N3 atoms has a mean plane deviation of 0.036 Å with the N1 showing the greatest displacement of 0.082 Å. The formally single C2–C3 bond (1.453(7) Å) which connects the thiosemicarbazone fragment to the rest of the molecule allows its free rotation, thus the dihedral angle formed between the best planes of the thiosemicarbazone fragment and the central pyrazole ring achieves 48.3°.

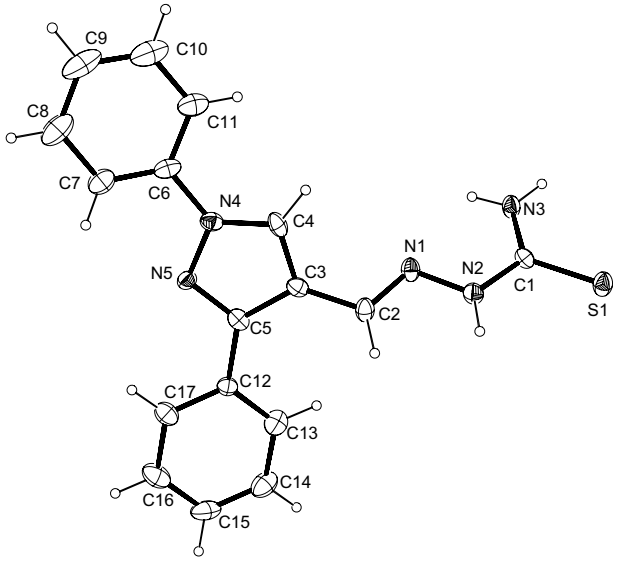

Fig. 2. Crystal structure of Ph_2PzTSC with the atomic numbering scheme. Ellipsoids are drawn at the 50% probability level.

Table 2
Selected bond lengths (Å) and angles (°)

	Ph_2PzTSC	$[Ni(Ph_2PzTSC\text{-}H)_2]$	
		A	B
Ni1–N1		1.914(3)	1.921(3)
Ni1–S1		2.141(2)	2.148(2)
N1–N2	1.387(5)	1.424(4)	1.410(4)
C1–N2	1.344(6)	1.289(5)	1.304(4)
C1–N3	1.315(6)	1.352(5)	1.349(4)
C1–S1	1.692(5)	1.744(4)	1.737(4)
C2–N1	1.279(6)	1.282(4)	1.296(4)
C2–C3	1.453(7)	1.449(5)	1.446(5)
N4–C5	1.432(7)	1.438(5)	1.435(5)
C5–C12	1.483(7)	1.470(5)	1.463(5)
N1–Ni1–S1		86.1(2)	85.51(9)
Ni1–N1–C2		128.3(3)	130.8(2)
Ni–N1–N2		117.7(2)	118.3(2)
Ni–S1–C1		94.4(2)	95.1(2)
N1a–Ni–N1b		102.5(2)	
S1a–Ni–S1b		90.1(1)	
N1a–Ni–S1b		162.9(3)	
N1b–Ni–S1a		163.8(3)	
N2–N1–C2	114.3(5)	113.9(3)	110.8(3)
N1–C2–C3	119.0(5)	124.3(3)	127.6(3)
N1–N2–C1	119.7(4)	110.9(3)	111.4(3)
N2–C1–S1	119.7(4)	123.9(3)	122.9(3)
N2–C1–N3	117.4(4)	119.4(4)	118.3(3)
N5–N4–C6	119.5(5)	120.5(3)	120.2(3)
N5–C5–C12	118.4(5)	119.4(4)	121.3(3)

The bond lengths within the aromatic parts of the molecule are normal [39]. The phenyl rings are titled in the same direction relative to the central pyrazole moiety. The dihedral angles formed between the best planes of the pyrazole and the two phenyl rings are similar, 18.1° and 19.1° with the C6–C11 and C12–C17 rings respectively. The dihedral angle between the titled phenyls is 6.0°.

The three intramolecular hydrogen bonds of the very bent character (D–H···A ≈ 100°) stabilize the geometry of Ph_2PzTSC (Table 3). The strongest intermolecular N3–H3···N5 hydrogen bond connects the centrosymmetrically related molecules into the cyclic dimers. Since this interaction is formed between the thiosemicarbazone and pyrazole moieties it probably causes the above mentioned twisting of the thiosemicarbazone fragment. The two interactions of the N–H···S type (Table 3) further connect the molecules of the ligand into the 2D structures parallel to the *ac* crystallographic plane. The segment of this 2D hydrogen bonded pattern is shown in Fig. 3.

3.5.2. Crystal structure of $[Ni(Ph_2PzTSC\text{-}H)_2]$

In $[Ni(Ph_2PzTSC\text{-}H)_2]$ complex the Ni(II) ion lies in an approximately square-planar coordination environment formed by two hydrazine N1 and two thiol S1 atoms from

Table 3
Geometry of hydrogen bonds

D–H···A	D–H (Å)	H···A (Å)	D···A (Å)	D–H···A (°)
Ph_2PzTSC				
N3–H3a···N1^{i}	0.86	2.29	2.642(2)	104.7(3)
C7–H7···N5^{i}	0.93	2.48	2.801(2)	100.1(4)
C17–H17···N5^{i}	0.93	2.53	2.836(2)	99.8(4)
N3–H3a···N5^{ii}	0.86	2.31	3.079(2)	140.1(3)
N2–H2n···S1^{iii}	0.86	2.68	3.312(4)	131.1(5)
N3–H3b···S1^{iv}	0.86	2.63	3.421(3)	155.2(5)
[Ni(Ph_2PzTSC-H)$_2$]				
C7a–H7a···N5a^{v}	0.93	2.57	2.853(2)	98.2(3)
C7b–H7b···N5b^{v}	0.93	2.54	2.830(2)	98.5(3)
C17a–H17a···N5a^{v}	0.93	2.61	2.883(2)	97.5(3)
C17b–H7b···N5b^{v}	0.93	2.67	2.930(2)	93.6(3)
N3a–H3a···N2a^{vi}	0.86	2.14	3.003(3)	178.3(3)
N3b–H3b···N2b^{vii}	0.86	2.12	2.968(2)	168.9(3)

Symmetry codes: (i) x, y, z; (ii) $-x+2$, $-y$, $-z+2$; (iii) $x+1.5$, y, $-z+2.5$; (iv) $x+0.5$, y, $-z+2.5$; (v) x, y, z; (vi) $-x$, $-y$, $-z+2$; (vii) $-x+1$, $-y$, $-z+1$.

the deprotonated thiosemicarbazone ligands (Fig. 4). The molecules of L have the *cis* mutual arrangement. The four donor atoms are significantly displaced from the mean coordination plane with the maximum deviation of atom N1a (0.471 Å).

The deviation from the regular square-planar geometry is also indicated by the coordination angles (Table 2). The N1a–Ni–N1b angle of 102.5(2)° shows significant disagreement with the theoretical value (90°) probably due to the steric effects between the bulky fragments attached to N1 atoms. The S1a–Ni–S1b angle shows almost ideal value of 90.1(1)°. The coordination bond distances Ni–N and Ni–S are comparable to those found in similar neutral square-planar complexes of Ni(II). Comparison of the remaining bonds in [Ni(Ph_2PzTSC-H)$_2$] to those of the uncoordinated ligand Ph_2PzTSC shows marked differences probably originated by the ligand's deprotonation and coordination. The most significant difference is found in the C–S bond which increases its length upon the ligand complexation for an average value of 0.048 Å. On the contrary, C1–N2 bond decreases its length for the similar average value.

Five membered chelate rings assume envelope conformation (the puckering parameters are: $q_2 = 0.324(3)$ Å, $\phi_2 = 181.0(7)°$, $q_2 = 0.320(2)$ Å, $\phi_2 = 182.5(7)°$ for the branches A and B respectively) and form the dihedral angle of 20.4°. The thiosemicarbazide moiety upon complexation retains its planarity, however it is worth mentioning that the dihedral angle between its best plane and central pyrazole ring decrease from the value of 48.3° to the values of 19.2° and 16.9° in the A and B branch respectively. This change in the ligand geometry is probably caused by the

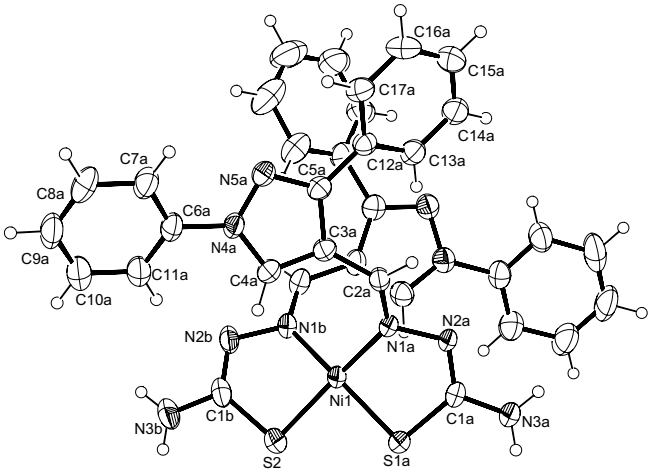

Fig. 4. Crystal structure of [Ni(Ph_2PzTSC-H)$_2$] with the atomic numbering scheme (the atomic numbering in the branch B is equivalent to A and is partly excluded for the sake of clarity). Ellipsoids are drawn at the 50% probability level.

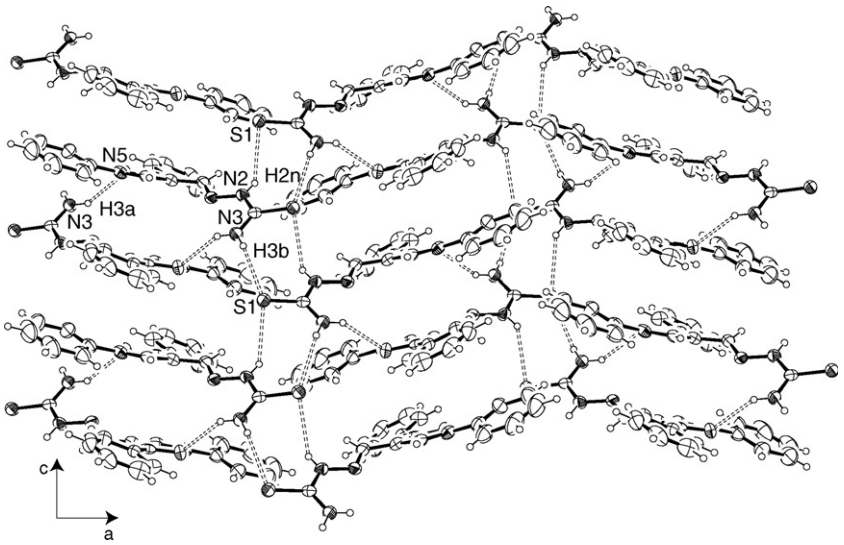

Fig. 3. View of the 2D hydrogen bonding linkage in Ph_2PzTSC.

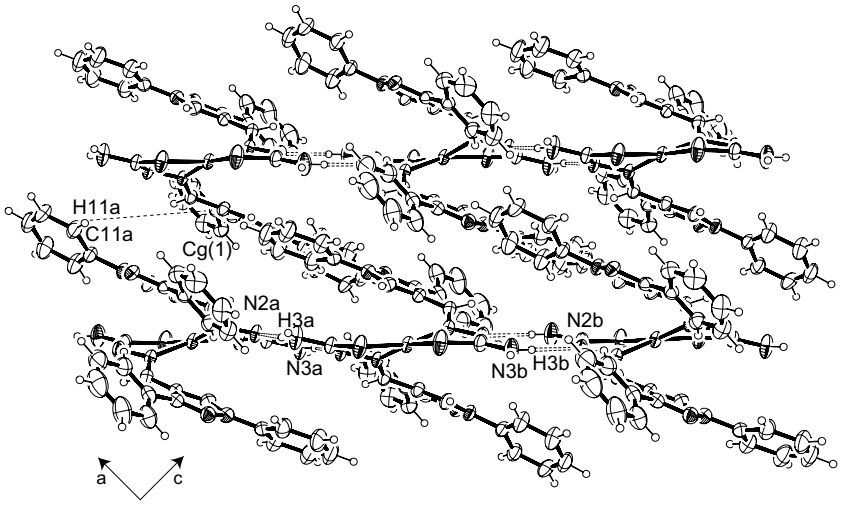

Fig. 5. Segment of the 2D molecular arrangement in [Ni(Ph_2PzTSC-H)$_2$].

braking of the N3–H3···N5 hydrogen bond, which plays a key role in the ligand's crystal arrangement. In the molecule of complex, the atom N5 remains only as an acceptor in the two intramolecular C–H···N bonds also present in the molecule of the free ligand (Table 3).

The molecules of complex are interconnected by the two pairs of N–H···N hydrogen bonds acting on each side of the molecule and connecting the [Ni(Ph_2PzTSC-H)$_2$] into the chains parallel to the diagonal of the *ac* plane. There is no further hydrogen bonding in this crystal structure; however the arrangement of the bulky carbonyl fragments provides the additional stabilizing contacts of the C–H···π type (C13a–H13a···Cg(1)^{i}: H13a···Cg = 2.92 Å, C13a–H13a···Cg = 140.1°; C11a–H11a···Cg(2)^{ii}: H11a···Cg = 2.88 Å, C11a–H11a···Cg = 137.1°; C17b–H17b···Cg(1)^{iii}: H17b···Cg = 2.99 Å, C17b–H17b···Cg = 102.3°. Cg(1) and Cg(2) are the centers of the rings N4b–C5b and C12a–C17a respectively. Symmetry codes: (i) x, y, z; (ii): $-x+1$, $-y$, $-z+2$; (iii) $-x$, $-y-1$, $-z+1$). It is interesting to notice that the dihedral angles formed between the central pyrazole moiety and the phenyl rings increase, compared to the corresponding angles in the ligand molecule (from 18.1° and 19.0° in HL to 27.0° and 27.2° (branch A) and 26.2° and 27.2° (B branch) of [Ni(Ph_2PzTSC-H)$_2$] respectively). However, in contrast to the branch B where the phenyl rings are as in the case of the ligand titled in the same direction regarding the pyrazole ring (the dihedral angle between the phenyls is 16.7°), in the A branch the phenyl rings are titled in the mutually opposite directions regarding the pyrazole (the dihedral angle between the phenyls is 49.3°). Namely, the C6a–C11a phenyl has the orientation which is different from those present in the free ligand and the branch B. It appears that in the absence of the other intermolecular interactions the C11a–H···π interaction in which this phenyl is involved has the decisive role in its final orientation. The segment of the 2D molecular arrangement is given in Fig. 5.

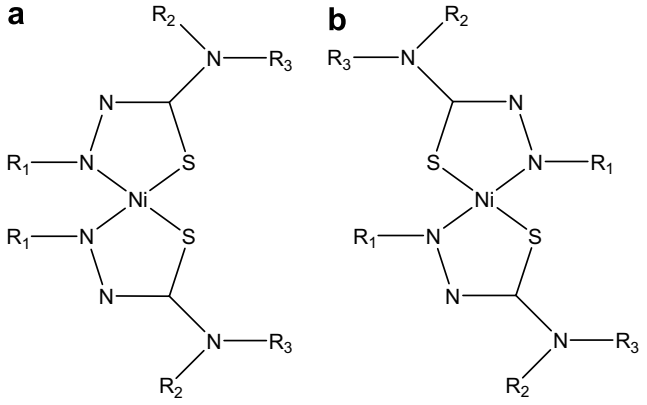

Fig. 6. Bis (bidentate) *cis*- and *trans*-Ni(II) complexes with thiosemicarbazide-based ligands.

3.5.3. Comparative database study of the similar bis(bidentate) Ni(II) complexes with the thiosemicarbazide-based ligands

As the X-ray analysis of [Ni(Ph_2PzTSC-H)$_2$] has shown, the square-planar geometry of this complex is rather tetrahedrally deformed (NNSS donor atoms deviate for 0.27 Å in average from the mean plane defined with these atoms). To compare its structural parameters and the coordination geometry to those of the similar bis(bidentate) Ni(II) complexes with the thiosemicarbazide-based ligands (Fig. 6) the CSD [40] search has been included. There are 37 crystal structures with the coordination number four extracted from the CSD and their refcodes are listed in Table 4.[1] The fact that only one (NIEPZF) of these structures shows the tetrahedral arrangement of the ligands can be explained by known preference of the Ni(II) ions to form square-planar complexes. From the remaining crystal structures, only

[1] List of references for all crystal structures extracted from CSD is given in the Supplementary material.

Table 4
Selected geometrical parameters for four-coordinated Ni(II) complexes with bidentate thiosemicarbazide-based ligands

Refcode[a]	P1/P2 (°)	Ni_P3 (Å)	Ni_P4 (Å)
NIEPZF	75.5	0.170	0.171
cis			
JEYPOS*	24.6	0.639	0.629
[Ni(Ph_2PzTSC-H)$_2$]*	22.7	0.602	0.596
XARWOC*	20.6	0.717	0.573
QEBDEG*	19.5	0.591	0.621
QEBDEG*	12.7	0.723	0.764
NIDTSS10	6.6	0.093	0.093
QEBDAC*	5.8	0.759	0.758
CNITSC	1.1	0.010	0.010
ALAHIE	0.2	0.112	0.074
WERNIQ	0.2	0.027	0.027
trans			
WUHQEV	4.2	0.491	0.191
XENNIN	3.9	0.249	0.162
BAKBUL	0.1	0.295	0.297
TCARNI01	0.0	0.213	0.213
EHAZOC	0.0	0.409	0.409
KUXLEU	0.0	0.232	0.232
ABECOA	0.0	0.108	0.108
ZOJXIF	0.0	0.089	0.089
BAKBIZ	0.0	0.219	0.219
RONDUT	0.0	0.419	0.419
WABHOX	0.0	0.277	0.277
BAKBOF	0.0	0.133	0.133
FIBWIX	0.0	0.205	0.205
TCARNI	0.0	0.198	0.198
FUTRAN	0.0	0.191	0.191
NIDTSS10	0.0	0.061	0.061
NIPTCZ10	0.0	0.008	0.008
BAKBEV	0.0	0.170	0.170
HOPCEU	0.0	0.386	0.386
VOGVIW	0.0	0.292	0.292
EHAZUI	0.0	0.146	0.146
EBEHEZ	0.0	0.351	0.351
KOMGAU	0.0	0.512	0.512
QOVGAJ	0.0	0.272	0.272
NSEMSU	0.0	0.002	0.002
ABECOA	0.0	0.133	0.133
FACKIE	0.0	0.569	0.569
IHAXAQ	0.0	0.445	0.445
TIFTUX	0.0	0.281	0.281
TNITSC	0.0	0.282	0.282

The complexes with the *cis*-positioned voluminous ligands are labeled by asterisk (*).

[a] List of references for all crystal structures extracted from CSD is given in the Supplementary material.

eight show the *cis* mutual arrangement (Fig. 6a) of the bidentate ligands, suggesting that this configuration is generally less favorable than *trans* (Fig. 6b). As expected, due to the steric hindrance the interligand N–Ni–N angle is larger in the *cis*-complexes with bulky carbonyl moieties attached to N donor atoms and it is ranging from 99.7° to 103.8°. Corresponding geometrical parameters calculated for [Ni(Ph_2PzTSC-H)$_2$] correlate very well with these values.

To compare the extent of the tetrahedral distortion on the same level (from the ideal square-planar geometry) in each of the listed complexes, we have analyzed the values of the dihedral angles formed between two N–Ni–S best planes. In Table 4. this angle is assigned as P1/P2. Because the N–Ni–S planes contain the central metal ion and a whole set of the donor atoms, the angle between them is sufficient to define the degree of the deformation of the coordination geometry from the ideal square-planar (P1/P2 = 0°) toward the tetrahedral one (P1/P2 = 90°). The structures in Table 4 are sorted with the reference to P1/P2 parameter. According to it the greatest deformations from the regular square-planar geometry are found in the complexes with the *cis*-positioned voluminous ligands as it is the case in the novel [Ni(Ph_2PzTSC-H)$_2$] which is the second most deformed. Interesting is the case of QEBDAC structure which exhibits somewhat less deformed square-planar geometry (P1/P2 parameter) but the most deformed chelate rings (based on parameters Ni_P3 and Ni_P4 which represent the displacement of the Ni atom from the best planes of the rest of the chelate rings). These observations suggest that there are two ways in which the geometry of the *cis*-Ni(II) square-planar complexes adopts to the requirements of the voluminous ligands: (1) through the distortion of the coordination geometry around the metal ion; (2) through the deformation of the preferentially planar five membered chelate rings.

It is evident that the *trans*-complexes have more regular square-planar geometry which is reflected in very low values of the P1/P2 parameter (Table 4) with NNSS donor atoms being practically in coplanar position. If voluminous substituents in these complexes exist they are also in *trans* position and from that reason they are not able to form intramolecular steric interactions. It seems however that in some cases (KOMGAU and FACKIE) they still affect the chelate rings conformation.

3.6. Thermal analysis

The decomposition curves of Ph_2PzTSC refer to the melting of the compound which is accompanied by its decomposition with an onset temperature of 490 K (217 °C). The fragmentation steps are superposed avoiding thus the determination of the decomposition mechanism. Some coke residue is observed in argon above 1000 K.

The decomposition of [Ni(Ph_2PzTSC-H)$_2$] begins at the same temperature (490 K) as that of the ligand with a low mass loss of about 2% (repeated measurements with samples from different synthesis). This means that the complex formation does not raise the thermal stability of the compound as is usual. On the basis of the mass loss, taking into account the short range interactions in the crystal, the leaving fragment is most probable an ammonia molecule (Calc. 2.4%). In IR spectrum of the intermediate the band of the original complex, assigned to $\nu(NH_2)$ vibration, has almost completely vanished, supporting the proposition of the departure of an ammonia molecule during the thermal decomposition up to 520 K. The deep purple color of the complex has also changed to dark brown.

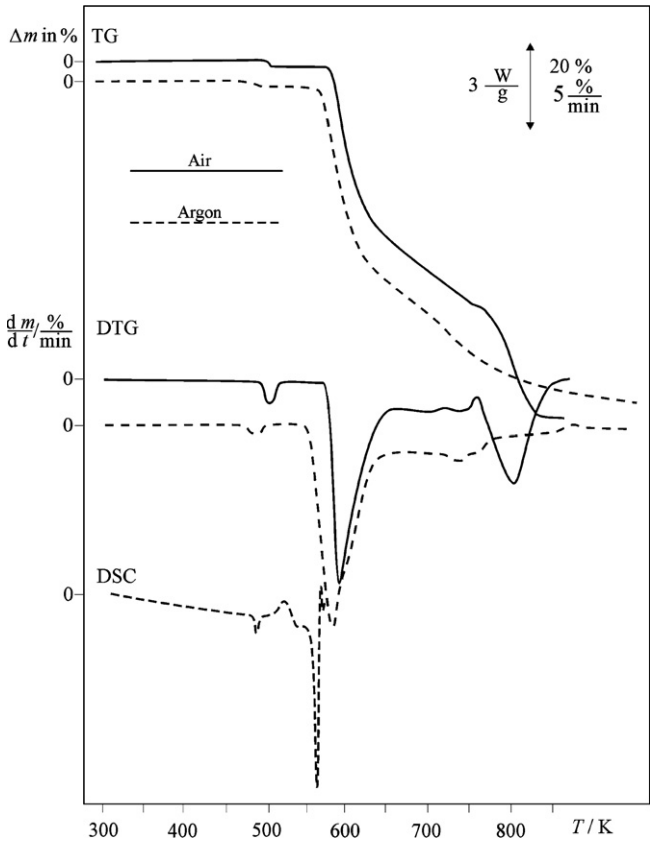

Fig. 7. Thermal decomposition curves of [Ni(Ph_2PzTSC-H)$_2$].

The mass loss is accompanied with an endothermic DSC peak which is followed by an exothermic one in a temperature range of 510–530 K. For this DSC peak no corresponding DTG peak is observed (see Fig. 7). Namely, in 510–560 K temperature range DTG curve falls to zero referring to formation of a stable intermediate. The exothermic process may be the consequence of a spontaneous intra- or intermolecular rearrangement [41], due to the loss of NH_3 molecule. According to the observation with a hot-stage microscope, there is no melting of the intermediate up to 550 K. The melting with an onset temperature at 550 K is immediately followed by an exothermic decomposition.

The decomposition of the complex begins at somewhat higher temperature in air, being continuous above 560 K in both atmospheres (Fig. 7). There is no possibility thus to determine the decomposition mechanism. As in sulfur containing complexes in air, in a platinum crucible, uncontrollable oxidation processes are taking place [42,43], it is meaningless to analyze the composition of the residue. In argon the decomposition is not finished up to 1000 K.

Acknowledgments

This work was supported by the Ministry of Science and Environmental Protection of the Republic of Serbia (Project No. 142028B) and the Provincial Secretariat for Science and Technological Development of Vojvodina.

Appendix A. Supplementary material

CCDC 633472 and 633473 contain the supplementary crystallographic data for Ph_2PzTSC and [Ni(Ph_2PzTSC-H)$_2$]. These data can be obtained free of charge via http://www.ccdc.cam.ac.uk/conts/retrieving.html, or from the Cambridge Crystallographic Data Centre, 12 Union Road, Cambridge CB2 1EZ, UK; fax: (+44) 1223-336-033; or e-mail: deposit@ccdc.cam.ac.uk. Supplementary data associated with this article can be found in the online version, at doi:10.1016/j.poly.2007.04.012.

References

[1] D.L. Klayman, J.F. Bartosevich, T.S. Griffin, C.J. Mason, J.P. Scovill, J. Med. Chem. 22 (1979) 855.
[2] D.X. West, S.B. Padhye, P.B. Sonawane, Struct. Bond. 76 (1991) 1.
[3] A.E. Liberta, D.X. West, Biometals 5 (1992) 121.
[4] F.A. French, E.J. Blanz, J.R. Do Amaral, D.A. French, J. Med. Chem. 13 (1970) 1117.
[5] H. Beraldo, D. Gambino, Mini. Rev. Med. Chem. 4 (2004) 31.
[6] W.L. John, R.M. Patera, M.J. Plummer, B.P. Halling, D.A. Yuhas, Pest. Sci. 42 (1994) 29.
[7] M.J. Genin, C. Biles, B.J. Keiser, S.M. Poppe, S.M. Swaney, W.G. Tarplay, Y. Yagi, D.L. Romero, J. Med. Chem. 43 (2000) 1034.
[8] H. Hashimoto, K. Imamura, J.I. Haruta, K. Wakitani, J. Med. Chem. 45 (2002) 1511.
[9] A.G. Habeeb, P.N.P. Rao, E.E. Knaus, J. Med. Chem. 44 (2001) 3039.
[10] M.L.P. Price, W.L. Jorgensen, J. Am. Chem. Soc. 122 (2000) 9455.
[11] R.R. Ranatunge, R.A. Earl, D.S. Garvey, D.R. Janero, L.G. Letts, A.M. Martino, M.G. Murty, S.K. Richardson, D.J. Schwalb, D.V. Young, I.S. Zemtseva, Bioorg. Med. Chem. Lett. 14 (2004) 6049.
[12] E. Elzein, R. Kalla, X. Li, T. Perry, E. Parkhill, V. Palle, V. Varkhedkar, A. Gimbel, D. Zeng, D. Lustig, D. Leung, J. Zablocki, Bioorg. Med. Chem. Lett. 16 (2006) 302.
[13] D.X. West, A.E. Liberta, S.B. Padhye, R.C. Chikate, P.B. Sonawane, A.S. Kumbhar, R.G. Yerande, Coord. Chem. Rev. 123 (1993) 49.
[14] A.K. Barik, S. Paul, S.K. Kar, R.J. Butcher, J.C. Bryan, Polyhedron 18 (1998) 571.
[15] N.C. Saha, R.J. Butcher, S. Chaudhuri, N. Saha, Polyhedron 22 (2003) 383.
[16] N.C. Saha, R.J. Butcher, S. Chaudhuri, N. Saha, Polyhedron 24 (2005) 1015.
[17] D.D. Perrin, W.L.F. Armarego, D.R. Perrin, Purification of Laboratory Chemicals, second ed., Pergamon Press, Oxford, 1980.
[18] P. Rathelot, N. Azas, H. El-Kashef, F. Delmas, C. Di Giorgio, P. Timon-David, J. Maldonado, P. Vanelle, Eur. J. Med. Chem. 37 (2002) 671.
[19] Enraf-Nonius CAD4 Software, Version 5.0, Enraf-Nonius, Delft, The Netherlands, 1989.
[20] CAD-4 Express Software. Enraf-Nonius, Delft, The Netherlands, 1994.
[21] (a) G.M. Sheldrick, SHELXS97. Program for the Solution of Crystal Structures, University of Göttingen, Germany, 1997;
(b) G.M. Sheldrick, SHELXL97. Program for the Refinement of Crystal Structures, University of Göttingen, Germany, 1997.
[22] (a) A.L. Spek, Acta Crystallogr., Sect. A 46 (1990) C34;
(b) A.L. Spek, PLATON, A Multipurpose: Crystallographic Tool, Utrecht University, Utrecht, The Netherlands, 1998.
[23] L.J. Farrugia, J. Appl. Crystallogr. 32 (1999) 837.
[24] M. Nardelli PARST, J. Appl. Crystallogr. 28 (1995) 659.
[25] L.J. Farrugia ORTEPIII for Windows, J. Appl. Crystallogr. 30 (1997) 565.
[26] Y. Tian, C. Duan, C. Zhao, X. You, Inorg. Chem. 36 (1997) 1247.

[27] M.R. Maurya, A. Kumar, M. Abid, A. Azam, Inorg. Chim. Acta 359 (2006) 2439.
[28] R.M. Silverstein, C.G. Bassler, T.C. Morrill, Spectrometric Identification of Organic Compounds, third ed., John Wiley and Sons Inc., New York, 1974, p. 113.
[29] P. Bera, N. Saha, S. Kumar, D. Banerjee, R. Bhattacharya, Transition Met. Chem. 24 (1999) 425.
[30] M.B. Ferrari, S. Capacchi, G. Reffo, G. Pelosi, P. Tarasconi, R. Albertini, S. Pinelli, P. Lunghi, J. Inorg. Biochem. 81 (2000) 89.
[31] P. Bindu, M.R.P. Kurup, T.R. Satyakeerty, Polyhedron 18 (1999) 321.
[32] E.M. Jouad, M. Allain, M.A. Khan, G.M. Bouet, Polyhedron 24 (2005) 327.
[33] E.M. Jouad, M. Allain, M.A. Khan, G.M. Bouet, J. Mol. Struct. 604 (2002) 205.
[34] M. Rodriguez-Argüelles, M.B. Ferrari, G.G. Fava, G. Pelizzi, G. Pelosi, R. Albertini, A. Bonati, P.P. Dall' Aglio, P. Lunghi, S. Pinelli, J. Inorg. Biochem. 66 (1997) 7.
[35] J.S. Casas, M.C. Rodriguez-Argüelles, U. Russo, A. Sanchez, J. Sordo, A. Vazquez-Lopez, S. Pinelli, P. Lunghi, A. Bonati, R. Albertini, J. Inorg. Biochem. 69 (1998) 283.
[36] M.R. Maurya, A. Kumar, A.R. Bhat, A. Azam, C. Bader, D. Rehder, Inorg. Chem. 45 (2006) 1260.
[37] M. Belicchi Ferrari, A. Bonardi, G. Gaspari Fava, C. Pelizzi, P. Tarasconi, Inorg. Chim. Acta 223 (1994) 77.
[38] A.B.P. Lever, Inorganic Electronic Spectroscopy, Russian Edition., Mir, Moscow, 1987, p. 2.
[39] M. Dincer, N. Ozdemir, I. Yildirim, E. Demir, Y. Akcamur, S. Isik, Acta Crystallogr., Sect. E 60 (2004) o317.
[40] F.H. Allen, Acta Crystallogr., Sect. B 58 (2002) 380.
[41] H.A. El-Boraey, J. Therm. Anal. Cal. 81 (2005) 339.
[42] K. Mészáros Szécsényi, V.M. Leovac, Ž.K. Jaćimović, G. Pokol, J. Therm. Anal. Cal. 74 (2003) 943.
[43] A. Kovács, D. Nemcsok, G. Pokol, K. Mészáros Szécsényi, V.M. Leovac, Ž.K. Jaćimović, I. Radosavljević Evans, J.A.K. Howard, Z.D. Tomić, G. Giester, New J. Chem. 29 (2005) 833.